OPEN ACCESS

CONTROL OF A HUMAN ARM EXOSKELETON USING AN ANALYTICAL APPROACH UNDER DIFFERENT INITIAL CONDITIONS AND SYSTEM PARAMETERS

Zahraa Abd Al-Elah Kahaleel[1] [0009-0009-1671-2719], Fawaz F. Al-Bakri[2] [0000-0003-1951-5402], Muslim Ali[3] [0000-0003-3785-6104]
[1]Mechanical Engineering Department, University of Kerbala, Iraq
[2]Department of Biomedical Engineering, College of Engineering, University of Babylon, Babylon, Iraq
[3]Prosthetics and Orthotics Engineering Department, College of Engineering, University of Kerbala, Iraq
Email: fawaz.al-bakri@uobabylon.edu.iq

Abstract - Exoskeletons have become an essential issue in our life to help people whose arms are immobile due to a stroke, muscle weakness, and neuromuscular disorders. One of these devices is a human arm exoskeleton. In this study, an efficient human arm exoskeleton controller has been designed to achieve a fast and stable response. To implement this design, the mathematical model of a human arm including five degrees of freedom is developed using the Lagrange–Euler methodology to analyse five displacements: hand, forearm, horizontal elbow, vertical elbow, and elbow angular displacements. Then the human arm system is linearized at a certain operating point to obtain a linear representation of the nonlinear system. Eight-term exponential functions are introduced to generate the five desired arm displacement profiles while preserving the elbow torque limitation and achieving initial, final, and intermediate boundary conditions. The initial boundary conditions are evaluated using a selected impulse input while the arm moves from rest. The final boundary conditions are determined under zero input as the arm returns to rest. While the intermediate conditions are proposed to ensure that the system captures the steady state conditions. Then the reference elbow torque is computed analytically using the predefined reference displacement profiles. Numerical simulations with different initial conditions and system parameters using Monte Carlo simulation technique are adopted to confirm the presented algorithm. The results demonstrated a rapid response, with a settling time of less than 0.25 seconds and completely without overshoot, under 1000 trials of initial displacements and system parameters variations.

Keywords: Human Arm Modelling, Analytical Approach, PD controller, Monte Carlo Simulation.

1. Introduction

One of the most fundamental components in mechanical systems is the control unit, which regulates the behaviour of mechanical systems by comparing the actual values of the system with reference values and generating a control signal that is applied to the system to minimize the difference between the two values. The work is characterized as a musculoskeletal system with two-degrees of freedom, where a controller was implemented by integrating DRNN with (GA) and the (EP) [1]. It was noted that DRNN is the best way to direct the human arm motion. In [2], [3] presented a PID tuning method by (PSO) to improve the time response of the system. MATLAB is used with virtual reality tools as it is easy to manipulate 3D objects defined using VRML. This study designed and built a 4DOF robot [4]. The controller used was an AT Mega 16 and a path continuous controller (PIC). ANSYS was used to formulate the finite-state method to calculate the displacement of the components. Solid Works Motion was used to design articulated robotic arms and mechanisms [5]. A six-degree-of-freedom robot arm was designed and controlled [6]. MATLAB Sim Mechanics was used. Laser pins were used to sense the gripper position.

The D-H. method and a PID controller were employed. The dynamics of a two-degree-of-freedom arm were modelled relying on the Lagrange-Euler method [7]. A PID controller was designed to control the robot arm to capture the desired joint angle by implementing and simulating the PID controller using MATLAB Simulink [8].

https://doi.org/10.17683/ijomam/issue22.v1.7

It was shown that even the minimal variation in the controller parameters leads to overshoot and increased fluctuations. On top of that, focused on the development of a two-degree-of-freedom PID control algorithm [9]. The traditional PID control method was improved to two degree of freedom PID control by introducing a fuzzy trapezoid. Likewise, a dynamic model of artificial muscles in an opposing pair organization for activating the elbow joint was presented [10]. The differential equations were solved using MATLAB using the Runge-Kutta method. In experimental assessments, the angular angles of the elbow joint were recorded, and the data were then analysed using MATLAB to determine the properties of the real system. A mechanical model of a robotic arm equipped with a pneumatic artificial muscle actuator for elbow therapy was studied [11]. The Lagrange-Euler method was used to demonstrate the robot dynamically with five degrees of freedom [12]. A PID controller was implemented using a PIDN pass filter, which improves control performance. A multi-jointed gravity-compensating exoskeleton was used for the arm. The range of motion in the joint space of four individual joints was assessed [13]. Similarly, an upper-limb exoskeleton was designed and developed for remote control of an industrial robot using an immersive environment [14]. A novel interactive technique based on hand gestures was introduced for 3D navigation in virtual environments. A seven-degree-of-freedom control scheme was used to control the upper-limb exoskeleton. However, a device was designed to control a human finger [15]. The tendon was modelled and controlled instead of motors with three degrees of freedom. Simulink was utilized for simulation. The results demonstrated that ASMC outperformed CSMC in reducing vibration and responding quickly. A field study was conducted, in which 39 plasterers were fitted with an exoskeleton during six weeks [16]. The work showed that 65% of plasterers expressed interest in using it and were enthusiastic about its load-reducing effect. This is the first job to introduce exoskeletons to an objective population and monitor their use. A machine learning computational approach was presented to process 12 channels of myoelectric signals from the shoulder and upper extremity [17], [18]. The reliability of the three machine learning algorithms was computed and compared to determine the optimal algorithm. An experiment was designed to test different levels of anti-gravity support using a passive upper limb exoskeleton, and its effects on electromagnetic signals were determined [18]. Average muscle activity was calculated over full and sub-cycles. Results showed that using the exoskeleton resulted in reduced electromagnetic activity across all muscles as opposed to the condition in which the exoskeleton system was not adopted.

The results showed that peak and mean levels of joint activation decreased linearly with increasing anti-gravity support provided by the upper limb exoskeleton [19]. In this study, a model of a prosthetic arm with five-degrees of freedom was examined. The Lagrange-Euler method was employed to derive the governing equations, and the model's analytical solution was obtained using MATLAB to analyse its dynamic behaviour and confirm the mathematical model. A PD controller was implemented to find the optimal torque needed for the motor to enable swift and stable movement of the arm. Additionally, Monte Carlo simulations were performed to assess the system's sensitivity to random parameter variations and to evaluate its performance across different operational scenarios.

Analytical control methodologies are a modern approach widely used in many engineering fields, including mechanical, electrical, and biomedical engineering due to the simplicity and non-singularity. In mechanical and electrical applications, [20 -25], utilized analytical functions to create the state references and compute the control command that used to equilibrate the system while pursuing the reference trajectories. While in biomedical applications, [26], [27] and [28], employed Fourier series function, second-order polynomial function, and seven-term exponential function to evaluate hip torque, antibiotic and, human knee torque, respectively. All of the analytical approaches successfully ensured the stability in a short time and with less overshot.

In this work, a human arm exoskeleton system is employed to rehabilitate a human arm. Firstly, the human arm model is derived using the Lagrange–Euler method. Secondly, the model is linearized at a certain operating point to obtain a linear representation of the nonlinear system. Then, Eight-term exponential functions are utilized to shape the reference system profiles while adhering to initial, final, and intermediate boundary conditions and ensuring the elbow torque does not exceed the maximum limit. In the end, the elbow torque is used to steer the human arm exoskeleton while including a wide range of initial displacements and system parameters.

2. Modeling Dynamic System

The human arm is modelled in Figure (1) as mass - damper- spring system which characterized by five degrees of freedom to describe the coordinates: z_1, z_2, z_3, y_1, θ. The angle $\tilde{\theta}$ denotes the nominal point of the upper arm, where vibrations will be studied around this certain position.

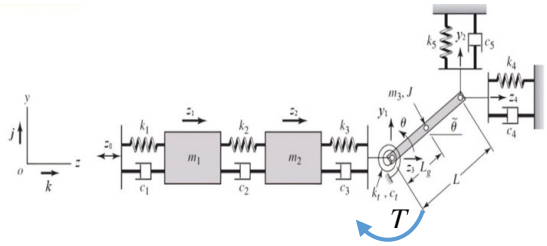

Figure 1: Human Arm System [29]

where z_1, z_2, z_3, y_1, and θ signify the hand, forearm, horizontal elbow, vertical elbow, and elbow angular displacements, respectively.

The z_0 denotes the external displacement that directly drives the hand segment. In addition, T represents the external elbow torque required to steer the human arm.

Table (1) lists the nominal human arm parameters [30]. These parameters were computed based on a Lagrangian multipliers methodology while maintaining fast convergence and minimal overshoot. The torsional stiffness in the shoulder joint is neglected due to its minor effect on the arm response.

Table 1. Nominal human arm parameters

Parameter	Value	Definition
m_1	0.4224 kg	Effective mass of the hand
m_2	1.1959 kg	Effective mass of the forearm segment
m_3	1.8074 kg	Mass of the upper arm
J	0.0149 kg.m^2	Rotational inertia of the elbow joint system
k_1	2.7517(10^4) N/m	Spring stiffness between ground and mass m_1
k_2	4.9795(10^4) N/m	Spring stiffness between m_1 and m_2
k_3	2.6602(10^5) N/m	Spring stiffness between m_2 and m_3
k_4	7.9757(10^3) N/m	Horizontal spring stiffness between trunk and point z_4
k_4	2.3470(10^4) N/m	Vertical spring stiffness between trunk and point y_2
k_t	5.2740(10^3) N/m	Torsional spring stiffness of the elbow
c_1	7.8376 N.s /m	Damper coefficient between ground and mass m_1
c_2	117.8178 N.s /m	Damper coefficient between m_1 and m_2
c_3	775.9501 N.s /m	Damper coefficient between m_2 and m_3
c_4	418.0506 N.s /m	Horizontal damper between trunk and point z_4
c_5	663.0399 N.s /m	Vertical damper coefficient between trunk and point y_2
c_t	80.4027 N.s /m	Torsional damper coefficient of the elbow
$\tilde{\theta}$	10 deg	Nominal position of the upper arm
L	0.29 m	Upper arm length
L_g	0.44 L m	Distance from the elbow to the upper arm

In the proposed system, there are three types of energy, consisting of kinetic energy, potential energy, and dissipated energy lost due to friction. The arm system produces kinetic energy owing to the movement of all arm segments. Thus, the total kinetic energy can be derived as presented below:

$$K_E = \frac{1}{2}m_1\dot{z}_1^2 + \frac{1}{2}m_2\dot{z}_2^2 + \frac{1}{2}m_3 \left\{ \begin{array}{l} \left[\dot{z}_3 - L_g\dot{\theta}\sin\left(\theta+\tilde{\theta}\right)\right]^2 \\ +\left[\dot{y}_1 + L_g\dot{\theta}\cos\left(\theta+\tilde{\theta}\right)\right]^2 \end{array} \right\} + \frac{1}{2}J\dot{\theta}^2 \quad (1)$$

The kinetic energy of the first two segments of the arm (hand and forearm) is produced during the horizontal motion, meanwhile the kinetic energy of the elbow joint is generated by horizontal and vertical motions as well as angular motion.

The potential energy represents the second source of energy which mainly depends on the effect of elastic and gravity forces. As illustrated in Fig.1, there are five elastic forces correspond to five mechanical springs and one gravity force arising from the elbow position with respect to the reference point. As a result, the overall potential energy is considered as:

$$P_E = \frac{1}{2}\begin{Bmatrix} k_1(z_1 - z_0)^2 + k_2(z_2 - z_1)^2 + \\ k_3(z_3 - z_2)^2 + k_t(\theta + \tilde{\theta})^2 + \\ k_4\left[z_3 + Lcos(\theta + \tilde{\theta})\right]^2 + \\ k_5\left[y_1 + Lsin(\theta + \tilde{\theta})\right]^2 \end{Bmatrix} + m_3 g[y_1 + L_g sin(\theta + \tilde{\theta}] \quad (2)$$

Continuously, the arm muscles have the ability to resist movement, which enables them to absorb energy and reduce oscillations. In the proposed system, energy is likely lost as a result of friction at the elbow joint; accordingly, the dissipated total energy might be represented as follows:

$$D_E = \frac{1}{2}\begin{Bmatrix} c_1\left(\dot{z}_1 - \dot{z}_0\right)^2 + c_2\left(\dot{z}_2 - \dot{z}_1\right)^2 + \\ c_3\left(\dot{z}_3 - \dot{z}_2\right)^2 + c_t\dot{\theta}^2 + \\ c_4\left[\dot{z}_3 - L\dot{\theta}\sin(\theta + \tilde{\theta})\right]^2 \\ + c_5\left[\dot{y}_1 + L\dot{\theta}\cos(\theta + \tilde{\theta})\right]^2 \end{Bmatrix} \quad (3)$$

As any mechanical engineering system, the human arm model undergoes the theory of conservation of energy.

The Euler-Lagrange method is selected here to describe the motion, taking into account the influence of kinetic, potential, and dissipated energies as illustrated in (Eq.4).

$$\frac{d}{dt}\left[\frac{\partial K_E}{\partial \dot{q}_i}\right] - \frac{\partial K_E}{\partial q_i} + \frac{\partial P_E}{\partial q_i} + \frac{\partial D_E}{\partial \dot{q}_i} = F_i \quad (4)$$

where q and i denote a system variable and number of degrees of freedom in the system, respectively. Applying the Euler-Lagrange method to determine the governing equations of motion.

Thus, the five-nonlinear equations of motion can be determined like so:

$$\begin{pmatrix} \left(\begin{matrix} m_1\ddot{z}_1 + (c_1 + c_2)\dot{z}_1 - c_2\dot{z}_2 + (k_1 + k_2)z_1 - k_2 z_2 \\ = c_1\dot{z}_0 + k_1 z_0 \end{matrix}\right) \\ \left(\begin{matrix} m_2\ddot{z}_2 + (c_2 + c_3)\dot{z}_2 - c_2\dot{z}_1 - c_3\dot{z}_3 + (k_2 + k_3)z_2 \\ -k_2 z_1 - k_3 z_3 = 0 \end{matrix}\right) \\ \begin{matrix} m_3[\ddot{z}_3 - L_g\cos(\theta + \tilde{\theta})\dot{\theta}^2 - L_g\sin(\theta + \tilde{\theta})\ddot{\theta}] \\ +(c_3 + c_4)\dot{z}_3 - c_3\dot{z}_2 - c_4 Lsin(\theta + \tilde{\theta})\dot{\theta} + \\ (k_3 + k_4)z_3 - k_3 z_2 + k_4 Lcos(\theta + \tilde{\theta}) = 0 \end{matrix} \\ \begin{matrix} m_3\left[\ddot{y}_1 - L_g\sin(\theta + \tilde{\theta})\dot{\theta}^2 + L_g\cos(\theta + \tilde{\theta})\ddot{\theta} + g\right] \\ +c_5\left[\dot{y}_1 + L\dot{\theta}\cos(\theta + \tilde{\theta})\right] + k_5\left[y_1 + Lsin(\theta + \tilde{\theta})\right] = 0 \end{matrix} \\ \begin{matrix} (J + m_3 L_g^{\,2})\ddot{\theta} + m_3 L_g \\ \left[-\ddot{z}_3 sin(\theta + \tilde{\theta}) + \ddot{y}_1 cos(\theta + \tilde{\theta})\right] + c_t\dot{\theta} \\ -c_4 L\sin(\theta + \tilde{\theta})\left[\dot{z}_3 - L\dot{\theta}\sin(\theta + \tilde{\theta})\right] + \\ c_5 L\cos(\theta + \tilde{\theta})\left[\dot{y}_1 + L\dot{\theta}\cos(\theta + \tilde{\theta})\right] + k_t(\theta + \tilde{\theta}) \\ -k_4 Lsin(\theta + \tilde{\theta})\left[z_3 + Lcos(\theta + \tilde{\theta})\right] + \\ k_5 Lcos(\theta + \tilde{\theta})\left[y_1 + Lsin(\theta + \tilde{\theta})\right] \\ +m_3 g L_g\cos(\theta + \tilde{\theta}) = T \end{matrix} \end{pmatrix} \quad (5)$$

In order to simplify the problem, the human arm system is linearized at a certain operating point to obtain a linear representation of the nonlinear system.

The linear model can be formulated as shown below:

$$\begin{pmatrix} m_1\ddot{z}_1+(c_1+c_2)\dot{z}_1-c_2\dot{z}_2+(k_1+k_2)z_1 \\ -k_2z_2=c_1\dot{z}_0+k_1z_0 \end{pmatrix}$$

$$\begin{pmatrix} m_2\ddot{z}_2+(c_2+c_3)\dot{z}_2-c_2\dot{z}_1-c_3\dot{z}_3 \\ +(k_2+k_3)z_2-k_2z_1-k_3z_3=0 \end{pmatrix}$$

$$\begin{pmatrix} m_3[\ddot{z}_3-L_g(cos\tilde{\theta}-\theta sin\tilde{\theta})\dot{\theta}^2- \\ L_g(\theta cos\tilde{\theta}+sin\tilde{\theta})\ddot{\theta}] \\ +(c_3+c_4)\dot{z}_3-c_3\dot{z}_2-c_4L(\theta cos\tilde{\theta}+sin\tilde{\theta})\dot{\theta} \\ +(k_3+k_4)z_3-k_3z_2+k_4L(cos\tilde{\theta}-sin\tilde{\theta})=0 \end{pmatrix} \quad (6)$$

$$m\begin{pmatrix} 3\begin{bmatrix} \ddot{y}_1-L_g(\theta cos\tilde{\theta}+sin\tilde{\theta})\dot{\theta}^2+ \\ L_g(cos\tilde{\theta}-\theta sin\tilde{\theta})\ddot{\theta}+g \end{bmatrix}+ \\ c_5\begin{pmatrix} \begin{bmatrix} \dot{y}_1+L\dot{\theta}(cos\tilde{\theta}-\theta sin\tilde{\theta} \end{bmatrix}+ \\ k_5\begin{bmatrix} y_1+L(\theta cos\tilde{\theta}+sin\tilde{\theta}) \end{bmatrix} \end{pmatrix}=0 \end{pmatrix}$$

$$\begin{pmatrix} (J+m_3L_g^{\,2})\ddot{\theta}+m_3L_g\begin{bmatrix} -\ddot{z}_3(\theta cos\tilde{\theta}+sin\tilde{\theta}) \\ +\ddot{y}_1(cos\tilde{\theta}-\theta sin\tilde{\theta}) \end{bmatrix} \\ +c_t\dot{\theta}-c_4L(\theta cos\tilde{\theta}+sin\tilde{\theta})\left[\dot{z}_3-L\dot{\theta}(\theta cos\tilde{\theta}+sin\tilde{\theta})\right] \\ +c_5L(cos\tilde{\theta}-\theta sin\tilde{\theta})\,[\dot{y}_1+L\dot{\theta}(cos\tilde{\theta}-\theta sin\tilde{\theta})] \\ +k_t(\theta+\tilde{\theta})-k_4L(\theta cos\tilde{\theta}+sin\tilde{\theta})\left[z_3+L(cos\tilde{\theta}-\theta sin\tilde{\theta})\right] \\ +k_5L(cos\tilde{\theta}-\theta sin\tilde{\theta})\left[y_1+L(\theta cos\tilde{\theta}+sin\tilde{\theta})\right] \\ +m_3gL_g(cos\tilde{\theta}-\theta sin\tilde{\theta})=T \end{pmatrix}$$

The arm equations can be formulated as a matrix representation where the mass, damping, and stiffness matrices are included as shown in Equation 7.

$$\begin{bmatrix} m_1 & 0 & 0 & 0 & 0 \\ 0 & m_2 & 0 & 0 & 0 \\ 0 & 0 & m_3 & 0 & -L_gm_3sin\tilde{\theta} \\ 0 & 0 & 0 & m_3 & L_gm_3cos\tilde{\theta} \\ 0 & 0 & -L_gm_3sin\tilde{\theta} & L_gm_3cos\tilde{\theta} & J+L_g^{\,2}m_3 \end{bmatrix}\begin{bmatrix} \ddot{z}_1 \\ \ddot{z}_2 \\ \ddot{z}_3 \\ \ddot{y}_1 \\ \ddot{\theta} \end{bmatrix}$$
$$+\begin{bmatrix} c_1+c_2 & -c_2 & 0 & 0 & 0 \\ -c_2 & c_2+c_3 & -c_3 & 0 & 0 \\ 0 & -c_3 & c_3+c_4 & 0 & -c_4Lsin\tilde{\theta} \\ 0 & 0 & 0 & c_5 & c_5Lcos\tilde{\theta} \\ 0 & 0 & -c_4Lsin\tilde{\theta} & c_5Lcos\tilde{\theta} & \begin{pmatrix} c_t+ \\ c_4L^2sin\tilde{\theta}^2 \\ +c_5L^2cos\tilde{\theta}^2 \end{pmatrix} \end{bmatrix}\begin{bmatrix} \dot{z}_1 \\ \dot{z}_2 \\ \dot{z}_3 \\ \dot{y}_1 \\ \dot{\theta} \end{bmatrix}$$
$$+\begin{bmatrix} k_1+k_2 & -k_2 & 0 & 0 & 0 \\ -k_2 & k_2+k_3 & -k_3 & 0 & 0 \\ 0 & -k_3 & k_3+k_4 & 0 & -k_4Lsin\tilde{\theta} \\ 0 & 0 & 0 & k_5 & k_5Lcos\tilde{\theta} \\ 0 & 0 & -k_4Lsin\tilde{\theta} & k_5Lcos\tilde{\theta} & \begin{pmatrix} k_t+k_4L^2 \\ \begin{pmatrix} cos\tilde{\theta}^2 \\ -sin\tilde{\theta}^2 \end{pmatrix} \\ +k_4L^2 \\ \begin{pmatrix} cos\tilde{\theta}^2 \\ -sin\tilde{\theta}^2 \end{pmatrix} \\ -m_3gL_gsin\tilde{\theta} \end{pmatrix} \end{bmatrix}\begin{bmatrix} z_1 \\ z_2 \\ z_3 \\ y_1 \\ \theta \end{bmatrix} \quad (7)$$
$$=\begin{bmatrix} c_1\dot{z}_0+k_1z_0 \\ 0 \\ -k_4Lsin\tilde{\theta} \\ -m_3g-k_5Lsin\tilde{\theta} \\ \left(-k_t\tilde{\theta}+k_4L^2sin\tilde{\theta}cos\tilde{\theta}-k_5L^2sin\tilde{\theta}cos\tilde{\theta}-m_3gL_gcos\tilde{\theta}\right)+T \end{bmatrix}$$

The initial and final states occur under static conditions where the arm is at a stable state. The initial displacements of the system can be determined by solving Equation 7, considering that both the velocity and acceleration are zero, and that no torque is applied at the elbow joint while applying a certain external displacement. The initial displacements can be computed using Eq. 8:

$$\begin{bmatrix} z_1 \\ z_2 \\ z_3 \\ y_1 \\ \theta \end{bmatrix}_0=\begin{bmatrix} k_1+k_2 & -k_2 & 0 & 0 & 0 \\ -k_2 & k_2+k_3 & -k_3 & 0 & 0 \\ 0 & -k_3 & k_3+k_4 & 0 & -k_4Lsin\tilde{\theta} \\ 0 & 0 & 0 & k_5 & k_5Lcos\tilde{\theta} \\ 0 & 0 & -k_4Lsin\tilde{\theta} & k_5Lcos\tilde{\theta} & \begin{pmatrix} k_t+k_4L^2 \\ \begin{pmatrix} cos\tilde{\theta}^2 \\ -sin\tilde{\theta}^2 \end{pmatrix} \\ +k_4L^2 \\ \begin{pmatrix} cos\tilde{\theta}^2 \\ -sin\tilde{\theta}^2 \end{pmatrix} \\ -m_3gL_g \\ sin\tilde{\theta} \end{pmatrix} \end{bmatrix}^{-1}$$
$$\times\begin{bmatrix} c_1\dot{z}_0+k_1z_0 \\ 0 \\ -k_4Lsin\tilde{\theta} \\ -m_3g-k_5Lsin\tilde{\theta} \\ -k_t\tilde{\theta}+k_4L^2sin\tilde{\theta}cos\tilde{\theta}-k_5L^2sin\tilde{\theta}cos\tilde{\theta}-m_3gL_gcos\tilde{\theta} \end{bmatrix} \quad (8)$$

In the same manner, the final displacements of the human arm can be determined under the same assumptions as the initial displacements, without considering the effect of external displacement. The final displacements can be computed using Eq. (9)

$$\begin{bmatrix} z_1 \\ z_2 \\ z_3 \\ y_1 \\ \theta \end{bmatrix}_f = \begin{bmatrix} k_1+k_2 & -k_2 & 0 & 0 & 0 \\ -k_2 & k_2+k_3 & -k_3 & 0 & 0 \\ 0 & -k_3 & k_3+k_4 & 0 & -k_4 L sin\tilde{\theta} \\ 0 & 0 & 0 & k_5 & k_5 L cos\tilde{\theta} \\ 0 & 0 & -k_4 L sin\tilde{\theta} & k_5 L cos\tilde{\theta} & \begin{pmatrix} k_t + k_4 L^2 \\ \begin{pmatrix} cos\tilde{\theta}^2 \\ -sin\tilde{\theta}^2 \end{pmatrix} \\ +k_4 L^2 \\ \begin{pmatrix} cos\tilde{\theta}^2 \\ -sin\tilde{\theta}^2 \end{pmatrix} \\ -m_3 g L_g sin\tilde{\theta} \end{pmatrix} \end{bmatrix}^{-1} \times \begin{bmatrix} 0 \\ 0 \\ -k_4 L sin\tilde{\theta} \\ -m_3 g - k_5 L sin\tilde{\theta} \\ -k_t\tilde{\theta} + k_4 L^2 sin\tilde{\theta} cos\tilde{\theta} - k_5 L^2 sin\tilde{\theta} cos\tilde{\theta} - m_3 g L_g cos\tilde{\theta} \end{bmatrix} \quad (9)$$

3. Analytical Controller Methodology

After deriving the model of the human arm, linearizing the nonlinear equations of motion at a specific operating point, and representing the model in matrix form [M, C, K, F], it becomes possible to design the elbow torque required to guide the human arm exoskeleton toward the desired steady state in a smooth manner. To carry this out, an analytical controller has been utilized to direct the exoskeleton following the desired reference trajectories. The reference trajectories of the system's displacements are shaped using five eight-term exponential functions, with one function designated for each displacement. This function is selected because it can produce smooth reference profile with no oscillations. Hence, the reference hand, forearm, horizontal elbow, vertical elbow, and elbow angular displacements, can be expressed in Eqs. (10,11,12, 13, and 14), respectively.

$$z_{1ref} = \sum_{n=1}^{8} A_n \exp(-1.5nt) \quad (10)$$

$$z_{2ref} = \sum_{n=1}^{8} B_n \exp(-1.5nt) \quad (11)$$

$$z_{3ref} = \sum_{n=1}^{8} C_n \exp(-1.5nt) \quad (12)$$

$$y_{1ref} = \sum_{n=1}^{8} D_n \exp(-1.5nt) \quad (13)$$

$$\theta_{ref} = \sum_{n=1}^{8} E_n \exp(-1.5nt) \quad (14)$$

Since each of Eqs. (10-14) consists of eight coefficients, eight boundary conditions must be imposed to solve for these coefficients. To perform this task, the initial, final, and intermediate displacements and velocities are used to generate the system's references while ensuring a fast response with no overshoot. For the hand segment, four pairs of displacement: (0, z10), (0.35, z1f), and (0.65, z1f), and four pairs of velocities: (0,z˙_10),(1,z˙_1f),(0.35,z˙_1f),and (0.65,z˙_1f) are significantly required at the initial, final, and intermediate states to compute the eight hand coefficients (A1, A2, A3, A4, A5, A6, A7, and A8). The hand displacement is considered as a representative case, and the other system displacements follow the same process to find the rest coefficients (Bn, Cn, Dn, En). Once computing the system's coefficients that define Eqs. (10-14), the first time derivative of Eqs. (10-14), and the second time derivative of Eqs. (10-14), it becomes straightforward to find the system's reference states and reference input. It is important to solve Eq. (7) in term of the elbow torque to obtain

$$\begin{aligned} T_{ref} = & -\ddot{z}_3 L_g m_3 sin\tilde{\theta} + \ddot{y}_1 L_g m_3 cos\tilde{\theta} + \left(J + L_g{}^2 m_3\right)\ddot{\theta} - \\ & c_4 L sin\tilde{\theta}\,\dot{z}_3 + c_5 L cos\tilde{\theta}\,\dot{y}_1 + \left(c_t + c_4 L^2 sin\tilde{\theta}^2 + c_5 L^2 cos\tilde{\theta}^2\right)\dot{\theta} \\ & -k_4 L sin\tilde{\theta} z_3 + k_5 L cos\tilde{\theta} y_1 + \\ & \left(k_t - k_4 L^2 \begin{pmatrix} cos\tilde{\theta}^2 \\ -sin\tilde{\theta}^2 \end{pmatrix} + k_5 L^2 \begin{pmatrix} cos\tilde{\theta}^2 \\ -sin\tilde{\theta}^2 \end{pmatrix} - m_3 g L_g sin\tilde{\theta}\right)\theta \\ & +k_t\tilde{\theta} - k_4 L^2 sin\tilde{\theta} cos\tilde{\theta} + k_5 L^2 sin\tilde{\theta} cos\tilde{\theta} + m_3 g L_g cos\tilde{\theta} \end{aligned} \quad (15)$$

Thus, substitute Eqs. (10-14) and the first- and second-time derivatives of Eqs. (10-14) into Eq. (15) to determine the time independent of the reference elbow torque required by the patient to achieve the desired movement

$$\begin{aligned} T_{ref} = & -2.25\sum_{n=1}^{8} n^2 C_n \exp(-1.5nt) L_g m_3 sin\tilde{\theta} \\ & +2.25\sum_{n=1}^{8} n^2 D_n \exp(-1.5nt) L_g m_3 cos\tilde{\theta} + 0.25 \\ & \left(J + L_g{}^2 m_3\right)\sum_{n=1}^{8} n^2 E_n \exp(-0.5nt) + 1.5 c_4 L sin\tilde{\theta} \\ & \sum_{n=1}^{8} nC_n \exp(-1.5nt) - 1.5 c_5 L cos\tilde{\theta}\sum_{n=1}^{8} nD_n \exp(-1.5nt) \\ & -0.5\left(c_t + c_4 L^2 sin\tilde{\theta}^2 + c_5 L^2 cos\tilde{\theta}^2\right)\sum_{n=1}^{8} nE_n \exp(-0.5nt) \\ & -k_4 L sin\tilde{\theta}\sum_{n=1}^{8} C_n \exp(-1.5nt) + k_5 L cos\tilde{\theta}\sum_{n=1}^{8} D_n \exp(-1.5nt) \\ & +\left(k_t - k_4 L^2 \begin{pmatrix} cos\tilde{\theta}^2 \\ -sin\tilde{\theta}^2 \end{pmatrix} + k_5 L^2 \begin{pmatrix} cos\tilde{\theta}^2 \\ -sin\tilde{\theta}^2 \end{pmatrix} - m_3 g L_g sin\tilde{\theta}\right) \\ & \sum_{n=1}^{8} E_n \exp(-0.5nt) + k_t\tilde{\theta} - k_4 L^2 sin\tilde{\theta} cos\tilde{\theta} \\ & +k_5 L^2 sin\tilde{\theta} cos\tilde{\theta} + m_3 g L_g cos\tilde{\theta} \end{aligned} \quad (16)$$

Figures (2-a)- (2f) display the reference hand displacement, forearm displacement, horizontal elbow displacement, vertical elbow displacement, elbow angular displacement, and elbow torque vs. time, respectively, under the nominal conditions for three excited displacements of (z0 =5 cm, z0 =15 cm, and z0 =25 cm). The findings demonstrate that an increase in the excited displacement causes higher initial magnitudes of all the states due to a higher stored energy. Furthermore, the reference profiles indicate that the analytical controller is reliable and the reference displacements profiles can be easily followed to capture the desired steady states even under varying initial displacements and system parameters, as will be discussed in the section that follows.

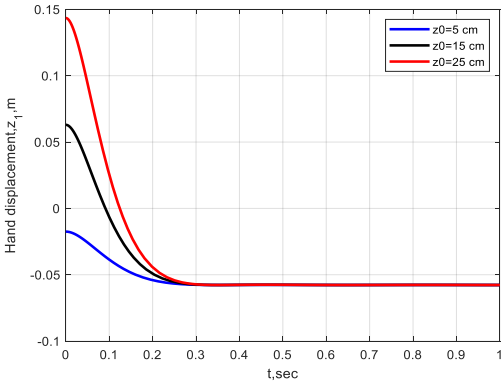

(a)

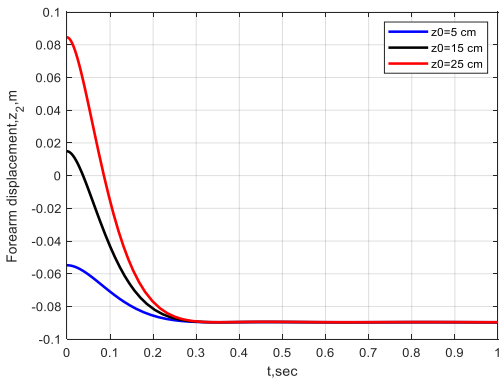

(b)

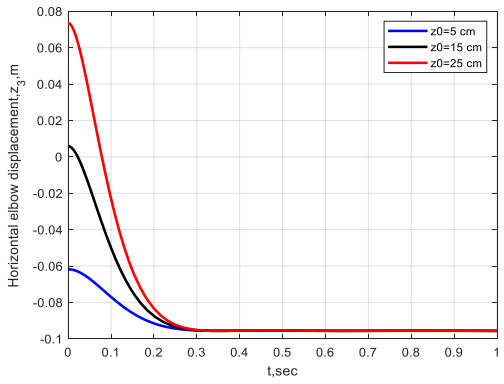

(c)

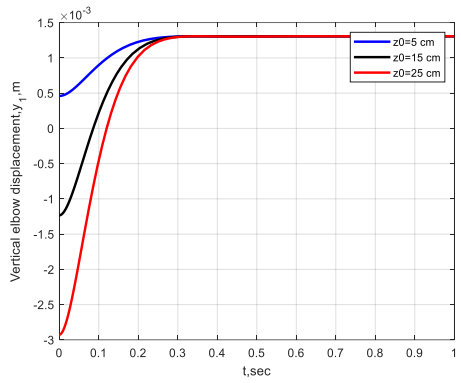

(d)

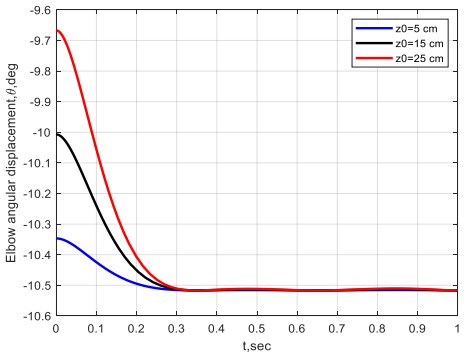

(e)

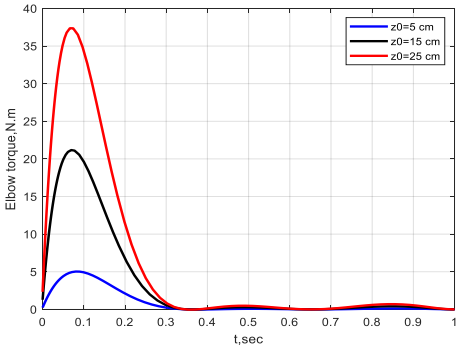

(f)

Figure 2: Reference displacements and elbow torque versus time under nominal conditions for three excited displacements; (a) hand displacement versus time; (b) forearm displacement versus. time; (c) horizontal elbow displacement versus time;(d) vertical elbow displacement versus time; (e) elbow angular displacement versus time; (f) elbow torque versus time

4. Numerical Simulation

The primary aim of arm exoskeleton algorithms is to direct the human arm to reach the steady state point in a short time while including the system input constraints. Usually, these procedures rely on two principles: producing a planned trajectory, then, a linear or nonlinear control approach is developed to follow the predefined reference trajectory.

In this work, in a completely different manner, the proposed controller can accurately steer the human arm effortlessly without requiring any feedback command. Consequently, in order to evaluate the effectiveness of the presented methodology, the arm exoskeleton system is numerically modeled within nominal conditions. In brief, Eq. (16) is the required elbow torque that will be used in Eq. (7) to follow the reference hand, forearm, horizontal elbow, vertical elbow, and elbow angular displacements characterized by Eqs. (10), (11), (12), (13) and (14), respectively.

Figures 3(a)-3(e), show the reference hand, forearm, horizontal elbow, vertical elbow, and elbow angular profiles vs. time, respectively under three different initial displacement 5cm, 15 cm, and 25 cm. With the application of the proposed analytical controller, Figs. (3b) and (3c) indicate that the exoskeleton system is highly capable of tracking the reference displacements. While Figs. (3a), (3d) and (3e) observe a well-suited agreement at steady state phase with minor discrepancies at the start due to the stronger nonlinearity of the elbow angle. On the whole, the presented results denote the capability of the analytical control to guide the exoskeleton arm swiftly within 0.35 sec without necessitating any additional feedback elbow torque.

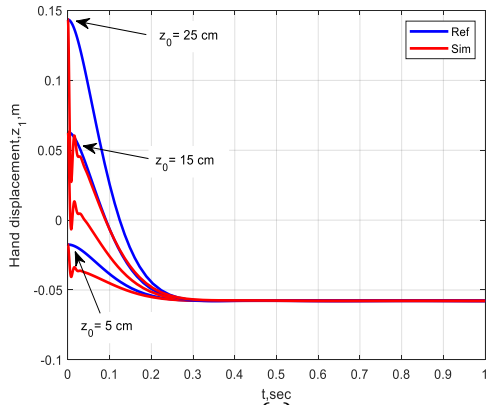

(a)

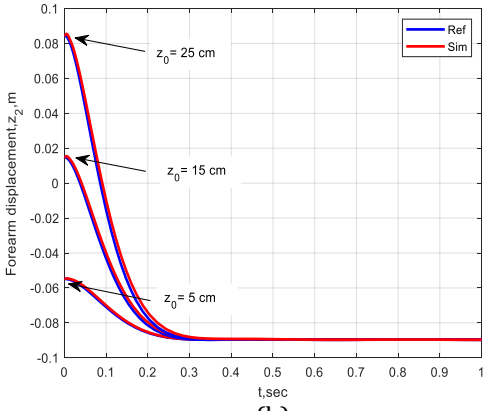

(b)

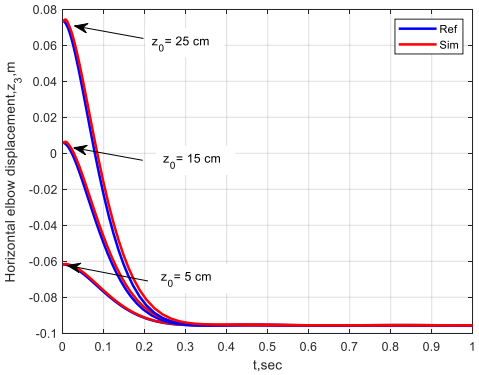

(c)

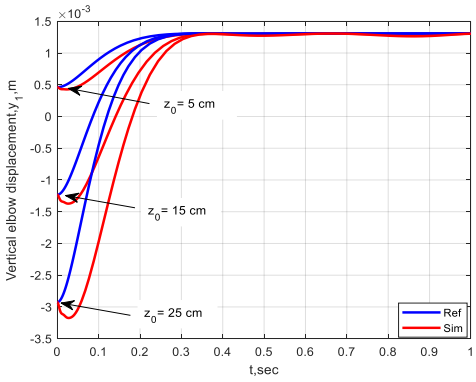

(d)

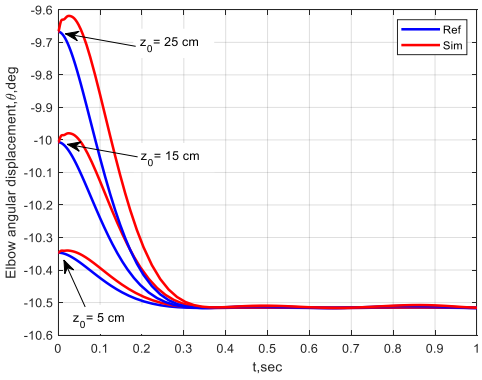

(e)

Figure 3 Reference and simulation displacements versus time under nominal conditions for three excited displacements; (a) hand displacement versus time; (b) forearm displacement versus. time; (c) horizontal elbow displacement versus time;(d) vertical elbow displacement versus time; (e) elbow angular displacement versus time

5. Monte Carlo Simulation

A Monte-Carlo approach is a procedure that exhibits variations in dynamic variables with precision [30] to [34]. With the use of this strategy, random variables are utilized per every path, depending on range of analyses.

To test the effeteness of the proposed algorithm, the statistics outcomes like the standard deviation, the minimum and maxim error, and mean value are recorded and the operation is occurred repeatedly with various income conditions.

In the introduced approach and in order to encompass a wide range of patient parameters, the Monte Carlo simulation method is conducted considering 1000 patients with variations in hand, forearm, and upper-arm masses, segment lengths, arm stiffness, and damping coefficients. These dispersions are modelled as random variations, with ((_-+)6%) added relative to the nominal conditions of each parameter to consider whether the rehabilitated arm belongs to a man, a woman, or a child.

Figures 4(a)-6(e), show histories of hand, forearm, horizontal elbow, vertical elbow, and elbow angular displacements errors and histories of the required elbow torque vs. time, respectively, for 1000 patients.

Figures 4(a) - 4(e) show that all the simulated displacements errors exhibit a fast decay during the first 0.25 sec and then the errors converge seamlessly to zero with no overshoot throughout the rest of simulation. Finally, Figure (4f) shows the elbow torque profiles remain below the maximum permissible value (< 60 N.m), which reveals that the arm exoskeleton may reach the desired steady state with no chance of system damage.

Figures 5(a)-5(f) show the statistical results of the hand displacement, forearm displacement, horizontal elbow displacement, vertical elbow displacement, and elbow angular displacement, and elbow torque errors, respectively, at the final position. It is observed from Fig. 5 that the final errors exhibit very small values despite a broad range of dispersions in the initial conditions and system parameters.

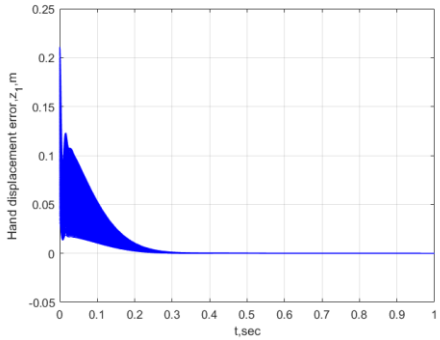

(a)

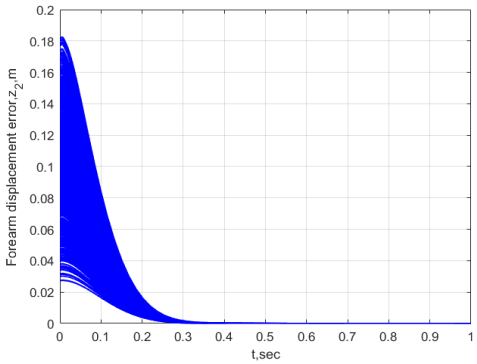

(b)

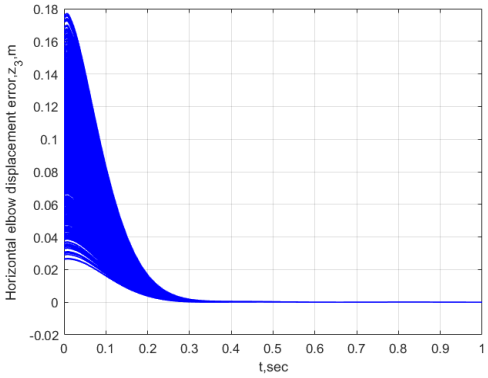

(c)

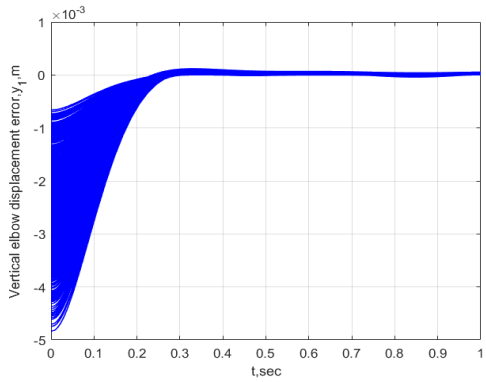

(d)

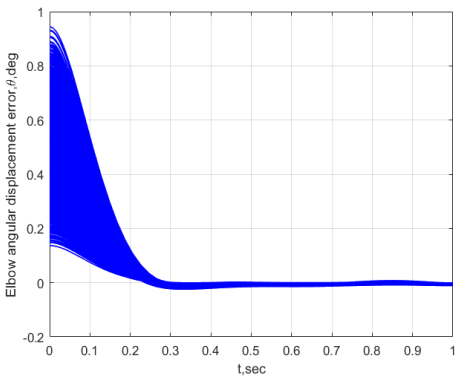

(e)

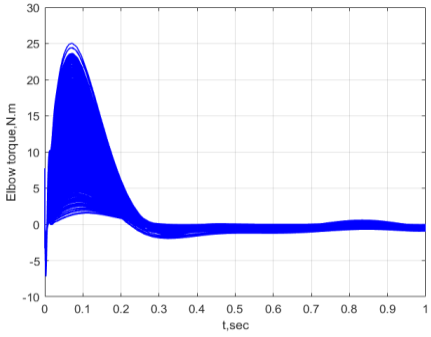

(f)

Figure 4. 1000 Human arm exoskeleton's histories versus time using analytical controller; (a) hand displacement error versus time; (b) forearm displacement error versus time; (c) horizontal elbow displacement error versus time;(d) vertical elbow displacement error versus time; (e) elbow angular displacement error versus time; (f) elbow torque error versus time.

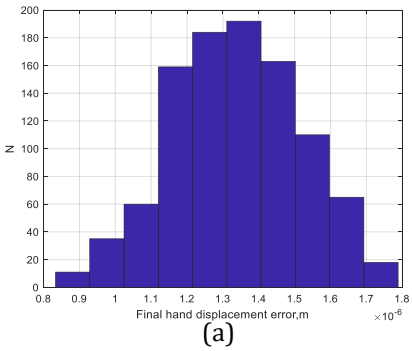

(a)

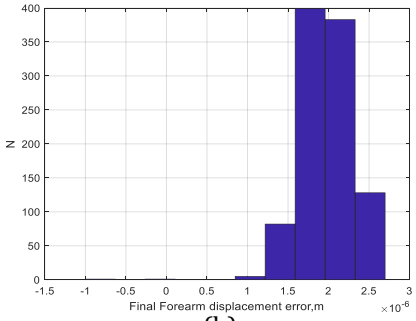

(b)

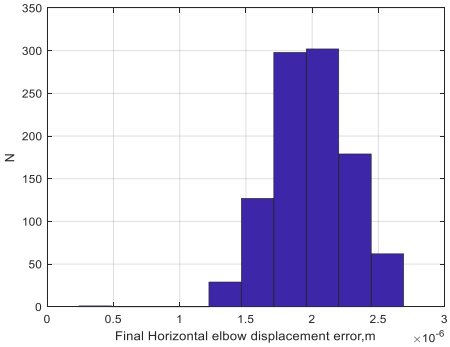

(c)

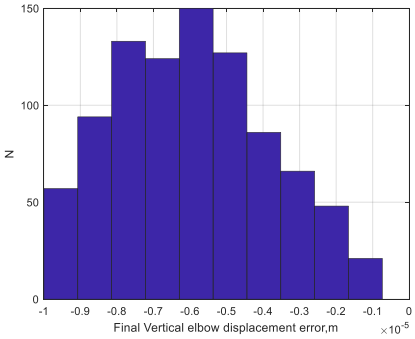

(d)

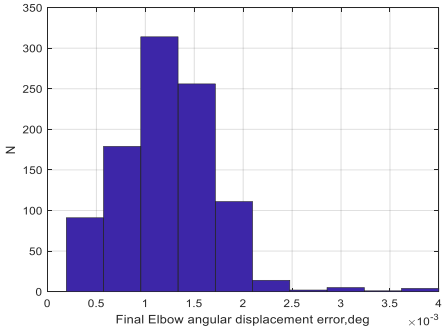

(e)

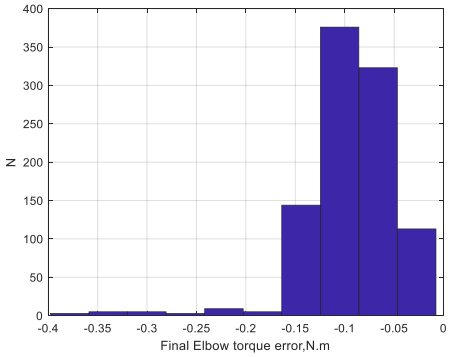

(f)

Figure 5 Statistics errors for the final system's states and input; (a) final hand displacement error; (b) final forearm displacement error; (c) final horizontal elbow displacement error ;(d) final vertical elbow displacement error; (e) final elbow angular displacement error; (f) final elbow torque error.

6. Conclusions

A new analytical strategy for the human arm exoskeleton has been introduced. The proposed controller was developed by means of the Eight-term exponential functions to describe the references of the system displacements. Considering the excited displacement, initial, final, and intermediate boundary conditions, the Eight-term analytical functions were solved in a linear manner to obtain the analytical elbow torque required to guide the arm exoskeleton from the starting state to the

required steady state. Numerical simulations with different initial conditions and system parameters were implemented to confirm the presented algorithm. A wide range of dispersions of hand, forearm, and upper-arm masses, segment lengths, arm stiffness, and damping coefficients with ((_-^+)6%) added to the nominal conditions have been conducted. The results revealed rapid convergence, ensuring steady state within 0.25 sec and zero overshoot in both system displacements and elbow torque without requiring any further feedback elbow torque. In addition, the statistical results illustrated that the steady-state errors remained very small with a maximum error of (4×10−3) deg in the elbow angle, a minimum error of (−1×10−5) m in the vertical elbow displacement, and a minimum elbow toque error as small as (-0.4) N.m even across 1000 patients.

References

[1] S. Liu, Y. Wang, and Q. Zhu, "Development of a new EDRNN procedure in control of human arm trajectories," *Neurocomputing*, vol. 72, no. 1–3, pp. 490–499, Dec. 2008, doi: 10.1016/j.neucom.2007.12.012.

[2] H. M. Mohammed Z. Al-Faiz, MIEEE, Abduladhem A. Ali, "Simulation of Digital Control of Human Arm Based PSO Algorithm in Virtual Reality," *Journal of Engineering and Development*, vol. 16, no. 3, pp. 126–138, 2012.

[3] M. A. Rashidifar, A. A. Rashidifar, and D. Ahmadi, "Modeling and Control of 5DOF Robot Arm Using Fuzzy Logic Supervisory Control," 2013. doi: 10.11591/ijra.v2i2.2974.

[4] M. Hassan and M. Baqar, "Design and Implementation of a DTMF Based Pick and Place Robotic Arm," *International Journal of Recent Research in Civil and Mechanical Engineering (IJRRCME)*, vol. 2, pp. 232–240, 2020, [Online]. Available: www.paperpublications.org

[5] Mohit Dhaka, Dr. Vikram Sharma, and Kaushal Khetan, "Control of Mechanisms and Robots using LabVIEW and SolidWorks and Arduino," *International Journal of Engineering Research and*, vol. V5, no. 02, Feb. 2016, doi: 10.17577/IJERTV5IS020312.

A. Nasr, A. E. Gaber, and H. A. El Gamal, "Design and Position Control of Arm Manipulator; Experimentally and in MATLAB SimMechanics." [Online]. Available: www.ijert.org

[6] Okubanjo, O. Oluwadamilola, O. Martins, and O. Olaluwoye, "Modeling of 2-DOF robot arm and control," *Futo Journal Series (FUTOJNLS)*, vol. 3, no. 2, pp. 80–92, 2017, [Online]. Available: www.futojnls.org

[7] N. M. Ghaleb and A. A. Aly, "Modeling and Control of 2-DOF Robot Arm," 2018.

[8] M. Bi, "Control of robot arm motion using trapezoid fuzzy two-degree-of-freedom PID algorithm," 2020. doi: 10.3390/SYM12040665.

A. Nikkhah, C. Bradley, and A. Sharif Ahmadian, "Design, dynamic modeling, control and implementation of hydraulic artificial muscles in an antagonistic pair configuration," 2020. doi: 10.1016/j.mechmachtheory.2020.104007.

[9] H. T. Nguyen, V. C. Trinh, and T. D. Le, "An adaptive fast terminal sliding mode controller of exercise-assisted robotic arm for elbow joint rehabilitation featuring pneumatic artificial muscle actuator," 2020. doi: 10.3390/act9040118.

[10] M. Salman, H. Khan, S. J. Abbasi, and M. C. Lee, "Dynamics Analysis and Control of 5 DOF Robot Manipulator," in *International Conference on Control, Automation and Systems*, IEEE, Oct. 2021, pp. 1705–1709. doi: 10.23919/ICCAS52745.2021.9649858.

[11] F. Grimm, J. Kraugmann, G. Naros, and A. Gharabaghi, "Clinical validation of kinematic assessments of post-stroke upper limb movements with a multi-joint arm exoskeleton," *J Neuroeng Rehabil*, vol. 18, no. 1, Dec. 2021, doi: 10.1186/s12984-021-00875-7.

[12] S. Kansal, M. Zubair, B. Suthar, and S. Mukherjee, "Tele-operation of an industrial robot by an arm exoskeleton for peg-in-hole operation using immersive environments," *Robotica*, vol. 40, no. 2, pp. 234–249, Feb. 2022, doi: 10.1017/S0263574721000485.

[13] H. Majeed, S. Kadhim, and A. Jaber, "Design of a Sliding Mode Controller for a Prosthetic Human Hand's Finger," *Engineering and Technology Journal*, vol. 40, no. 1, pp. 257–266, Jan. 2022, doi: 10.30684/etj.v40i1.1943.

A. W. de Vries, S. J. Baltrusch, and M. P. de Looze, "Field study on the use and acceptance of an arm support exoskeleton in plastering," *Ergonomics*, vol. 66, no. 10, pp. 1622–1632, 2023, doi: 10.1080/00140139.2022.2159067.

B. Chen *et al.*, "Volitional control of upper-limb exoskeleton empowered by EMG sensors and machine learning computing," *Array*, vol. 17, Mar. 2023, doi: 10.1016/j.array.2023.100277.

[14] G. Ramella, L. Grazi, F. Giovacchini, E. Trigili, N. Vitiello, and S. Crea, "Evaluation of antigravitational support levels provided by a passive upper-limb occupational exoskeleton in repetitive arm movements," *Appl Ergon*, vol. 117, May 2024, doi: 10.1016/j.apergo.2024.104226.

[15] L. Grazi *et al.*, "Passive shoulder occupational exoskeleton reduces shoulder muscle coactivation in repetitive arm movements," *Sci Rep*, vol. 14, no. 1, Dec. 2024, doi: 10.1038/s41598-024-78090-2.

[16] Al-Bakri, F.F., Ali, H.H. and Khafaji, S.O.W., 2024. Adaptive control of a submarine for various

diving depths using an exponential function. *Jurnal Teknologi (Sciences & Engineering)*, *86*(4), pp.79-86.

[17] Ali, H.H., Khafaji, S.O.W., Al-Bakr, F.F. and Aubad, M.J., 2024. DESIGN OF A MOTION CONTROL FOR A HYDRAULIC ROTARY ACTUATOR USING A VARIABLE DISPLACEMENT PUMP. International Journal of Mechatronics and Applied Mechanics, (18), pp.60-66.

[18] Lami, S.K., Bakri, F.F., Ali, H.H. and Khafaji, S.O.W., 2024. Forward control of an electromagnetic actuator using an exponential approach. International Journal of Mechatronics and Applied Mechanics, (15), pp.15-22.

[19] Ali, H.H., Al-Bakri, F.F. and Khafaji, S.O.W., 2023. Analytical position control system of a linear hydraulic actuator used in aircraft applications. International Journal of Mechatronics and Applied Mechanics, (13), pp.209-218.

[20] Al-Bakri, F.F., Ali, H.H. and Waheed, K.S.O., 2021. A new analytical control strategy for a magnetic suspension system under initial position dispersions. FME Transactions, 49(4), pp.977-987.

[21] Al-Bakri, F.F., Khafaji, S.O.W. and Ali, H.H., 2021. A novel analytical control of a single rotary inverted pendulum under initial angular dispersions. International Journal of Mechatronics and Applied Mechanics, (10), pp.32-42.

[22] Вахид, Х.С.О., 2025. УПРАВЛЕНИЕ ЭЛЕМЕНТАМИ ЭКЗОСКЕЛЕТА С ИЗМЕНЕНИЕМ ПАРАМЕТРОВ РЯДОВ ФУРЬЕ ДЛЯ АДАПТИВНОЙ РЕАБИЛИТАЦИИ ПАЦИЕНТОВ. Российский журнал биомеханики, 29(1), pp.54-64.

[23] Al-Bakri, F.F., Ali, H.H., Al Humaish, S.S.H. and Khafaji, S.O.W., 2024, August. An Analytical Methodology for Controlling Hepatitis B Virus Infection with Uncertain Patient Parameters. In International Conference on Reliable Systems Engineering (pp. 140-151). Cham: Springer Nature Switzerland.

[24] Al-Bakri, F.F., Khafaji, S.O.W., Ali, H.H., Al Juboori, A.M. and Cihan, I.H., 2024. A new nonlinear analytical control of the human knee joint of paraplegic patients under initial knee angle uncertainties. International Journal of Mechatronics and Applied Mechanics, (17), pp.16-22.

[25] Balachandran, B. and Magrab, E.B., 2018. *Vibrations*. Cambridge University Press.

[26] Abd Al-Elah Kahaleel, Z., Al-Bakri, F.F. and Ali, M., 2025, September. Dynamic Response of a Human Arm Model Using Lagrangian Multipliers Method Under Various Input Displacements. In International Conference on Reliable Systems Engineering (pp. 83-98). Cham: Springer Nature Switzerland.

[27] Khafaji, S.O.W., Ali, H.H., Al-Bakri, F.F. and Manring, N.D., 2025, September. Controlling a Magnetorheological (MR) Fluid Brake by Simultaneously Adjusting the Electrical Current and the Fluid-Film Thickness. In International Conference on Reliable Systems Engineering (pp. 133-149). Cham: Springer Nature Switzerland.

[28] Al-Bakri, F.F., Lami, S.K., Ali, H.H. and Khafaji, S.O.W., 2021, September. A sliding mode control of an electromagnetic actuator used in aircraft systems. In 2021 5th Annual Systems Modelling Conference (SMC) (pp. 1-5). IEEE.

[29] Al-Bakri, F.F., Khafaji, S.O.W., Ali, H.H. and Muhi, L.N., 2021, January. Adaptive model predictive control for a tora system under initial axial and angular position dispersions. In 2021 IEEE 11th Annual Computing and Communication Workshop and Conference (CCWC) (pp. 1294-1299). IEEE.

[30] Ali, H.H., Khafaji, S.O.W. and Al-Bakri, F.F., 2021. H∞ loop shaping control design of the rotational velocity of a hydraulic motor. Internation

[31] Laheeb, M., Salwan, K., Fawaz, A.B. and Sarah, L., 2018, January. Online algorithm for controlling a cruise system under uncertainty in design parameters and environmental conditions using Monte-Carlo simulation. In 2018 IEEE 8th Annual Computing and Communication Workshop and Conference (CCWC) (pp. 424-430). IEEE.

[32] Fawaz, A.B., Laheeb, M. and Salwan, K., 2018, January. Online algorithm for controlling an inverted pendulum system under uncertainty in design parameters and initial conditions using Monte-Carlo simulation. In 2018 IEEE 8th Annual Computing and Communication Workshop and Conference (CCWC) (pp. 1-7). IEEE.